Optical and Quantum Electronics **23** *(1991) 1–27*

TUTORIAL REVIEW

Surface plasmon–polaritons and their uses

KEVIN WELFORD
Royal Signals and Radar Establishment, Malvern, Worcestershire, WR14 3PS, UK

Surface plasmon–polaritons have been experimentally and theoretically studied for many years but in recent years interest has grown substantially due to their possible use in novel device applications. The aim of this review is to introduce the concept of surface plasmon–polaritons so that the reader will be able to appreciate the physics they can probe, and the device applications in which they may be utilized.

1. Scope of the article

There are many ways of exciting surface plasmon–polaritons (SPPs) using either electron beams or photons on planar, rough, or grating surfaces. Historically, electron beam excitation was first used, with optical excitation being introduced in the late 1960s. To put the historical aspects into perspective the reader is directed to the classic review by Raether [1]. By far the most versatile technique of exciting SPP's in planar geometries is the method of attenuated total reflection (ATR), which was independently demonstrated by Otto [2], and Kretschmann and Raether [3], albeit in slightly different forms. In this review we will concentrate on the ATR method of excitation. Although Otto, and Kretschmann and Raether, are credited with establishing the ATR method of exciting SPPs, it is a technique first demonstrated by Turbadar [4] some years earlier. Really, the major contribution from Otto was to establish that the excited mode in this type of ATR technique was the SPP.

Although SPPs are the most widely investigated type of surface polaritons, there are many different forms. Readers interested in a broader perspective of the topic are directed to texts edited by Boardman [5] and Agranovich and Mills [6]. A recent book by Raether [7] and a short review by Sambles [8] are also recommended.

2. Introduction

Let us begin with the phenomenon of total internal reflection (TIR). Electromagnetic radiation incident on an interface from a higher, n_1, to a lower, n_2, refractive index medium will, beyond the critical angle θ_c, be totally reflected, see for example Harrick [9], and Hirschfield [10]. If a third medium, of high refractive index, n_3, is placed within the exponentially decaying fields, a propagating wave may again be excited. Photon 'tunnelling' can be thought to have occurred from medium 1 to medium 3, across a low refractive index barrier. This situation is schematically represented in Fig. 1. Arranging for $n_1 > n_3$ ensures that $\theta_1 < \theta_3$. This allows the full range of wavevectors, parallel to the interface, to be accessed in medium 3 for a reduced angle range in medium 1. With both media 1 and 3

0306–8919/91 $03.00 + .12

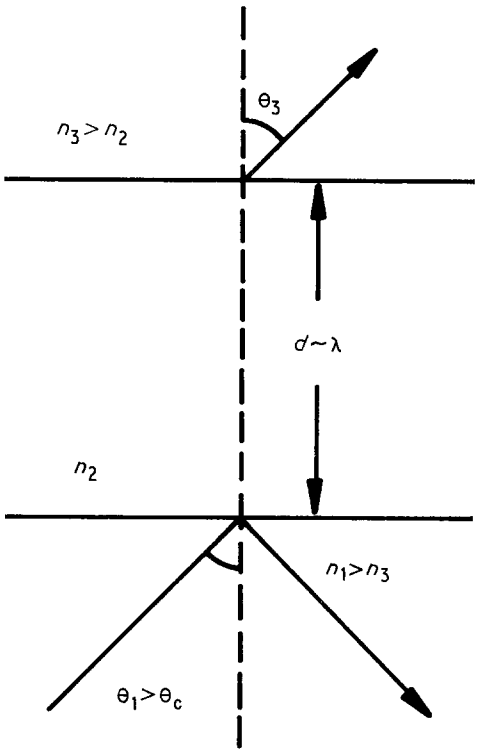

Figure 1 A coupling layer of thickness d and refractive index n_2 sandwiched between two semi-infinite media with refractive indices n_1 and n_3.

semi-infinite, the incident and transmitted wave propagation angles, θ_1 and θ_3 respectively, are simply related by Snell's law. A more interesting situation occurs when medium 3 is thin, with a thickness of the order of the wavelength of light. Electromagnetic energy reflected from the second surface of medium 3 will interfere with the driving field, and only at specific angles will energy be transferred into the thin dielectric layer. This phenomena is well known in integrated optics, see Tien [11] for a review. When the phase-matching condition is satisfied, which depends on the refractive indices of each medium, and the thickness of medium 3, energy is transferred from the incident wave to a guided wave, confined to propagate within medium 3, resulting in a drop in the reflected wave intensity, see Fig. 2. Two features of interest appear in the theoretical reflected intensity. First, there is the critical angle, labelled θ_c, at which point the fields in the air become exponentially decaying. Secondly, there are a series of reflectivity minima, labelled $m = 0, 1, 2, 3$, which indicate that phase matching to guided wave modes occurs at these angles. In this present example TM, or p-polarised, incident radiation has been considered. Although each of the guided modes corresponds to energy being transferred from the incident field to the waveguide, the distribution of the energy within the waveguide differs from mode to mode. For the guided mode $m = 0$ the energy is transported predominantly in the centre of the waveguide, falling off toward the boundaries, and exponentially decaying in the adjacent media. Although the exact details of the energy flow differ for each of the guided modes, they all share the common feature that energy is confined to propagate between boundaries.

If one alters the tunnelling gap material from a dielectric to a metal, such as silver, a new reflection minimum is observed, indicating that an additional mode can be excited (see Fig. 3). This additional mode is the surface plasmon–polariton (SPP). In order to appreciate

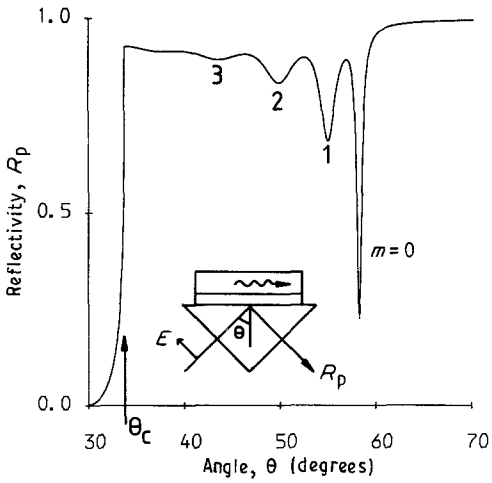

Figure 2 Reflected intensity as a function of angle of incidence for p-polarised light, demonstrating phase matching to four guided waves, schematically drawn in inset figure is the experimental system. The critical angle, θ_c, is indicated.

how this mode differs from the guided waves, it is most instructive to calculate the Poynting vector field at the incident angle corresponding to phase-matching to the SPP, see Fig. 4. Energy is transported at the interface between the metal and dielectric layers. Removing the dielectric layer would not prevent the SPP mode from being excited, since it is the metal surface that is of importance here, but the phase-matching condition to the SPP would be altered. The thickness of the metal layer has been carefully chosen to ensure strong coupling to the SPP. Two features of the SPP should be noted from its Poynting vector field distribution. Firstly, the electromagnetic fields at the metal surface are much larger than those in the incident field. Secondly, the fields decay exponentially perpendicular to the interface. A consequence of these exponentially decaying fields is that the mode is non-radiative; it cannot directly couple into a propagating photon field, or be excited directly by an incident light wave. What has been demonstrated here is the ATR technique of optically exciting SPPs. By using the evanescent field within the metal layer, the wavevector of the incident light can be increased beyond its free space value, allowing a phase match to the SPP. If the metal layer is illuminated with TE, or s-polarised, light a different reflectivity is found. Although the critical angle and the four guided modes are still excited,

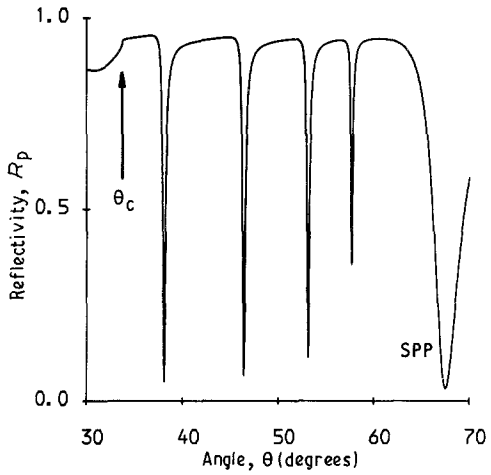

Figure 3 Reflected intensity as a function of angle of incidence for p-polarised light demonstrating excitation of SPP, when the coupling gap is made of silver.

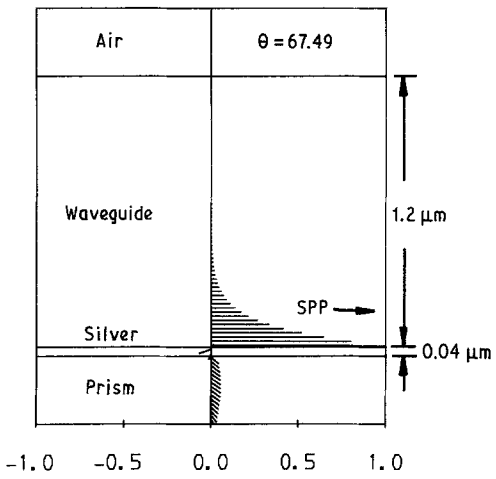

Figure 4 Poynting vector field for SPP showing surface field enhancements.

at slightly different incident angles, the SPP is not excited. The reason for this is straightforward. A discontinuity of the electric field component, perpendicular to the metal surface, generates a surface charge density at the interface which can then couple to the photon field forming the SPP; only TM radiation has a non-zero perpendicular electric field component.

In an intuitive fashion we have seen that SPPs are a special class of guided waves. Propagation distances of a bulk guided wave are much greater than the SPP since the latter loses energy via Joule heating. Strong field localization and enhancement means that the phase matching condition is sensitive to the dielectric properties at, or very close to, the interface. The majority of the interest in SPP excitation arises from these properties. Similarities between guided waves and SPP are explored further by Swalen [12].

3. Properties of surface plasmon–polaritons

There are many different forms of surface polariton. As an electromagnetic wave propagates through a polarisable medium, the polarisation it induces modifies the wave and the electromagnetic wave becomes coupled to the induced polarisation. This coupled excitation is called a polariton. If the wave is bound to a surface then it is referred to as a surface polariton. When the polarisable medium is identified, the polariton can be qualified. In the case of interest in this article, the polarisable system is a free electron gas and so the surface polariton is called a surface plasmon–polariton (SPP). Alternatively, the polarisation of the medium could have been due to the phonon system, in which case, it would be referred to as a surface phonon-polariton. There are a range of other types of polariton, and the interested reader is directed towards references [5] and [6] for more details. It is the dielectric properties of the active medium which determine which type of polariton is supported. One of the media at the interface, along which the surface wave propagates, is referred to as 'active' and the other 'passive'. All this tells us is which of the two media has the dielectric properties that cause the wave to be found to the interface. In the next section it will be shown that the active medium causes the wave to be bound to the surface by having the real part of the relative permittivity negative. Therefore, at a metal–dielectric interface it is the metal that is the surface active medium.

Throughout the literature the terms SPP and surface plasmon (SP) are used almost interchangeably. Strictly, there is a difference. When the surface wavevector, k, is greater

than ω_p/c, where ω_p is the plasma frequency, defined in Equation 4 below, and c is the speed of light, the electromagnetic wave is sufficiently mismatched from the induced polarisation for limited coupling to occur. Under these conditions, called the non-retarded limit, the system can be described using electrostatics and the surface wave is then a surface plasmon. Conversely, when $k < \omega_p/c$, strong coupling between the electromagnetic wave and the induced polarisation occurs and the surface wave is then a SPP. This is referred to as the retarded limit. Bulk plasmons correspond to the familiar plasma oscillations that occur at an angular frequency of ω_p. The result that a surface plasmon has a reduced angular frequency, $\omega_p(2)^{-1/2}$ at a metal–vacuum interface, was first theoretically discussed by Ritchie [13]. This result is modified if the passive medium has a non-unity relative permittivity. Since that time a range of confirmatory experiments have been performed, leading to the excitation of SPPs using ATR in the retarded limit by Otto.

3.1. Single interface

There are many ways to establish the dispersion relations for surface modes, see for example Ritchie and Edridge [14], Kliewer and Fuchs [15, 16], Otto [2], and Burstein *et al.* [17]. A route more appropriate to this article is that originally proposed by Cardona [18], and subsequently discussed by other authors such as Kovacs [19], Welford [20], and Boardman [21].

Consider a single interface between two media with relative permittivities ε_1 and ε_2, where the active medium is chosen to be medium 2. Applying Maxwell's equations, the relationships between the amplitudes of the incident electric field, E_i, the reflected electric field, E_r, and the transmitted electric field, E_t, can be described using Fresnel's equations. For p-polarised light the relationship between the incident and reflected electric field amplitudes is given by;

$$\frac{E_r}{E_i} = \frac{\varepsilon_1 k_{2z} - \varepsilon_2 k_{1z}}{\varepsilon_1 k_{2z} + \varepsilon_2 k_{1z}} \tag{1}$$

where ε_i is the dielectric constant in the ith medium and;

$$k_{iz} = (\varepsilon_i(\omega^2/c^2) - k_x^2)^{1/2}$$

is the normal wavevector component of the ith medium. In this expression k_x is the wavevector component parallel to the interface, ω is the angular frequency and c the velocity of the electromagnetic wave in vacuum.

For a surface wave solution of Maxwell's equations, only one field may exist in each medium, a point emphasised by Fano [22]. From Equation 1 this means that either E_i or E_r need to be set to zero. This leads to a pair of dispersion relations;

$$\begin{aligned} \varepsilon_1 k_{2z} &= \varepsilon_2 k_{1z} \qquad \text{with } E_r = 0 \\ \varepsilon_1 k_{2z} &= -\varepsilon_2 k_{1z} \qquad \text{with } E_i = 0 \end{aligned} \tag{2}$$

These two dispersion equations are both solutions of the more general single interface dispersion relation;

$$k_x^2 = \frac{\omega^2}{c^2}\left(\frac{\varepsilon_1 \varepsilon_2}{\varepsilon_1 + \varepsilon_2}\right) \tag{3}$$

It was Fano [22] who pointed out that the difference between the two bound surface modes arises due to the sign of the dielectric function of the active medium. For the

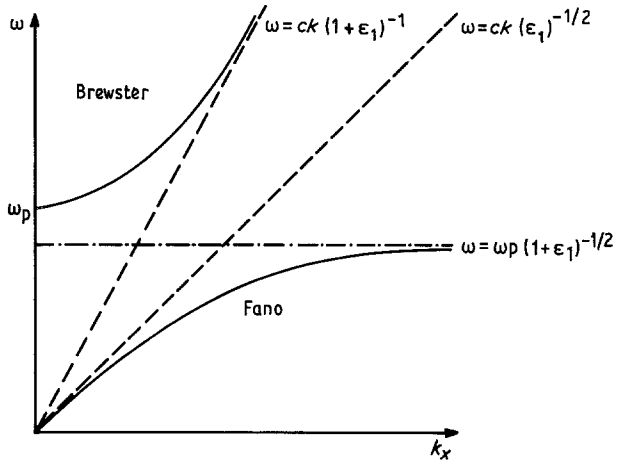

Figure 5 Dispersion curves for single interface surface modes illustrating asymptotic limits.

purposes of the discussion here it will be assumed that both ε_1 and ε_2 are real, hence the media exhibit no loss, and ε_2 is described by the free electron expression;

$$\varepsilon_2(\omega) = 1 - \frac{\omega_p^2}{\omega^2} \tag{4}$$

where

$$\omega_p^2 = \frac{4\pi ne^2}{m}$$

is the plasma frequency, e, the electronic charge, m, the electron mass and, n the electron density. (Limitations of using this dielectric relative permittivity for the metal are that it begins to fail whenever contributions to the electronic structure arise from other sources, such as d-band contributions in gold at short visible wavelengths. Generally, it holds more accurately at longer wavelengths, remote from ω_p. Also, this particular form of the relative permittivity does not include any damping term. Surface wave solutions that it implies are free to propagate unattenuated, and thus cannot be excited.) As the frequency, ω, of the optical field is varied the free electron dielectric response changes sign. For the region where $\omega > \omega_p$ we have that $\varepsilon_2 < 0$, in which case the latter dispersion relation in Equation 2 applies, and when $\omega > \omega_p$, the value of $\varepsilon_2 > 0$, and then the former dispersion relation in Equation 2 applies. Substituting the dielectric function of the surface active medium into the dispersion relation, the dispersion of k_x with frequency, ω, can be plotted for both the high and low frequency modes. This has been done in Fig. 5. In this figure the asymptotic gradients are shown, see Boardman [21]. The high frequency mode turns out to be the familiar Brewster condition, see for example Welford [20] or Boardman [21]. Because the surface wavevector of the incident light can always be made large enough to match the Brewster condition, by altering the angle of incidence, direct coupling to the Brewster mode is achievable. This is a consequence of k_{1z} and k_{2z} being real. In fact this mode can show a bound form when a small imaginary term is introduced into the dielectric permittivity, Halevi [23].

In the frequency interval

$$\omega_p > \omega > \omega_p/(1 + \varepsilon_1)^{1/2}$$

no propagating surface wave solutions exist because k_x becomes imaginary. This can be seen by inspection of Equation 3 and the form of the free electron relative permittivity.

When $\omega < \omega_p/(1 + \varepsilon_1)^{1/2}$, the value of k_x again becomes real, and a new type of surface mode is excited, called the Fano mode. Under these conditions, both k_{2z} and k_{1z} are imaginary, and of opposite sign. Fields perpendicular to the interface decay exponentially into either medium, but wave propagation occurs along the interface. When $\theta_1 = 90°$ the wave vector of the incident light along the interface has its maximum value of;

$$k_{1x}|_{max} = \frac{\omega}{c}(\varepsilon_1)^{1/2}$$

Even at grazing incidence, the incident wave vector is not large enough to match the surface wave vector of the Fano mode. For the single interface system this mode cannot be excited directly. A Fano mode propagating along the interface is essentially trapped from decaying into an unguided wave and is said to be a non-radiative mode. In a real metal the dielectric constant is complex and the oscillating electric charges lose energy via Joule heating. The surface wave corresponding to this situation exhibits an exponentially decaying amplitude, along the interface, and is the SPP. Detecting the excitation of the SPP by measuring the temperature increase of the metal can be achieved, see Innes and Sambles [24]. Propagation of a SPP along a rough metal surface, leads to a further loss mechanism, that of roughness coupled re-radiation. Extra momentum required to convert the surface wave into free space photons can be made up by the Fourier components of the roughness profile. If the intensity profile of the re-radiated light is recorded as a polar intensity diagram information can be extracted about the root mean square roughness of the interface. A review of this phenomena can be found in Raether [1], and recent experimental work can be found in Barnes and Sambles [25]. Experimentally, provided that care is taken in preparing the metal surface the effects of roughness can largely be ignored.

Exponential decay of the electromagnetic fields away from the metal–dielectric interface is one of the exploitable properties of SPP. Dielectric permittivity changes close to the interface acutely affect the propagation of the surface wave, dramatically altering its dispersion properties. It is this attribute of the SPP that is exploited in modulator and sensor device applications. But how far do these fields extend away from the interface? Typical decay lengths into metals are 12 nm for aluminium and 22 nm for silver. The typical decay lengths into vacuum are $\approx 0.3\,\mu$m, in the blue and $1.5\,\mu$m in the red.

In order to excite this surface wave it is necessary to increase the momentum of the incident light waves and one technique used to achieve this is to introduce a second interface. This leads directly to the technique of attenuated total reflection (ATR).

3.2. Double interface

Consider a double interface system, where the three media are labelled 1, 2 and 3. Medium 2 is sandwiched between media 1 and 3. Either by following the calculations made by Ward *et al.* [26], or the later treatment by Burstein *et al.* [17], or by introducing the boundary condition directly into the two interface Fresnel's equation, following the procedure of

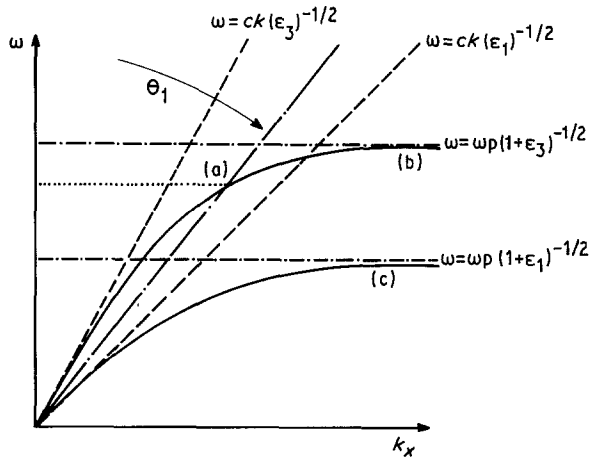

Figure 6 Dispersion curves for double interface surface modes with dissimilar semi infinite media.

Cardona [18], it is possible to calculate the double interface surface wave dispersion relation. This is schematically plotted in Fig. 6 following, for example, Abeles [27]. A study of three media systems, involving semiconducting materials, was made by Holm and Palik [28] in which a detailed discussion is given of the interrelationship between dispersion relations, ATR, and reflectivity. Fig. 6 is, in some sense, just the single interface dispersion curve repeated for both semi-infinite dielectrics. We see that the asymptotic limits have the same form as before. From Fig. 6, it is clear that incident radiation can now couple to the portion of the dispersion curve labelled (a), that is between the two lines with gradients $c(\varepsilon_3)^{-1/2}$ and $c(\varepsilon_1)^{-1/2}$, provided the coupling angle θ_1 is chosen correctly. When θ_1 increases so that k_{1x} crosses the line with gradient $c(\varepsilon_3)^{-1/2}$

$$\sin\theta_1 = (\varepsilon_3/\varepsilon_1)^{1/2}$$

which is the condition for total internal reflection in medium 1. When θ_1 reaches its maximum value of 90°, k_{1x} will have increased to lie on the line with gradient $c(\varepsilon_1)^{-1/2}$. This shows that the electromagnetic fields in media 2 and 3 are evanescent and the fields in medium 1 are oscillatory. The evanescent fields in media 2 and 3 both exponentially decay away from the interface. If medium 1 is a glass prism, medium 2 air, and medium 3 a metal, light incident in the prism at some particular angle, θ_{spp}, which depends on the frequency of the light, will excite a SPP-like mode at the metal–air interface. This phase matching condition is illustrated in Fig. 6 by the horizontal dotted line intercepting the dispersion curve, labelled a. This is the method of ATR excitation first demonstrated in 1968 by Otto [2], and later modified by Kretschmann and Raether [3], making medium 2 a thin film of metal, directly evaporated on to the prism. These two ATR techniques, see Fig. 7, form the basis for all optical excitation of SPP in planar systems today. Although the presence of the coupling prism perturbs the dispersion of the SPP from that expected for a single interface the effect maybe fully taken into account by a multilayer Fresnel's equation calculation, see Kovacs [19], which can be formulated more concisely using 2 × 2 matrix methods. A beautiful demonstration of the dispersion curve of the SPP in the visible has been given by Swalen *et al.* [29].

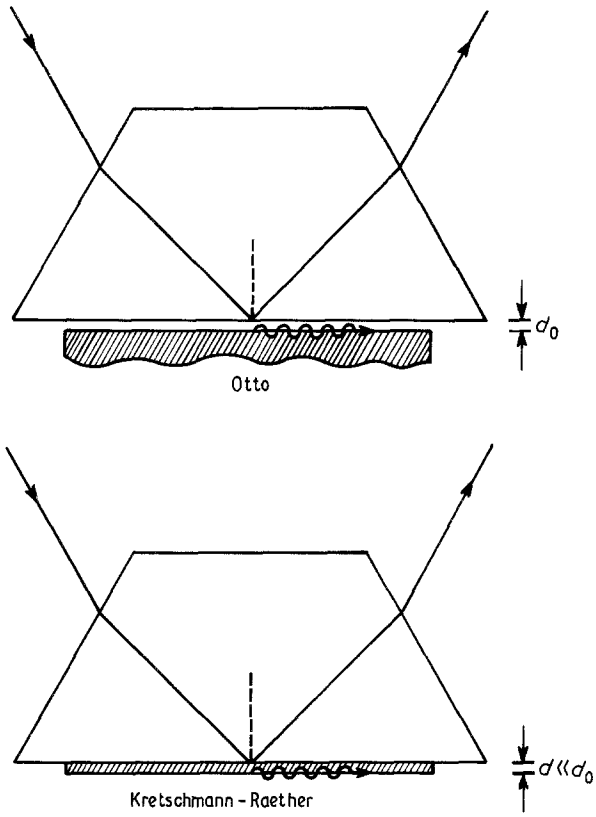

Figure 7 The two prism coupling methods used in SPP excitation. In the Kretschmann–Raether geometry the metal thickness for optimum coupling, d, is much less than the air gap thickness for optimum coupling d_0 in the Otto geometry.

4. Dielectric properties of metals

One of the simplest measurements that can be made using SPPs is of the dielectric constant of the surface active medium. Investigating the dispersion of the dielectric constant of silver is by far the most frequent. Primary reasons for this are that silver is relatively inert, does not degrade too readily when exposed to air, or a range of fluids, and the ATR resonance is narrow and approximately Lorentzian throughout the visible range.

A recent study of silver, in which the metal surface is in contact with air and various liquid dielectrics, has been conducted by Gugger *et al.* [30]. In this work a high index prism with the metal film evaporated on to the hypotenuse face that is, the Kretschmann–Raether configuration, is encased in a cell, into which liquid maybe introduced, and placed on to a computer controlled rotating table. A beamsplitter is used to provide a reference beam, which allows monitoring of the incoming light. Once the light has been reflected from the metal film it is collected by a second detector, which is rotating at twice the rate of the prism, in order to keep track of the reflected beam. Because of refraction at the air–prism boundaries the reflected beam does not rotate simply at twice the rate of the prism, but is also linearly translated. For wide angle scans this can mean the reflected beam moves a significant amount over the detector surface which in some cases can cause problems. Narrow half-width resonances, exhibited by silver in the visible, typically $\approx 0.7°$, do not

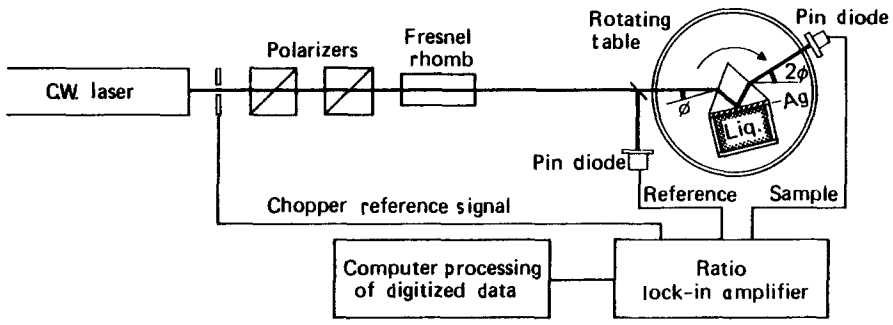

Figure 8 Typical experimental set up for angle scanned ATR measurement of SPP using a goiniometer mechanism, after Gugger *et al.* [30]. Computer control affords rapid and accurate data aquisition.

pose this problem. A typical experimental arrangement as used by Gugger *et al.* [30], is shown in Fig. 8. Monitoring the critical angle as part of the reflected spectrum allows the refractive index of the prism to be accurately measured. Correcting the reflected signal for reflection losses at both of the prism–air entrance and exit interfaces, the theory can be matched to data using the real and imaginary parts of the dielectric constant and the film thickness as the only fitting parameters.

Investigation of the thin film properties of gold using the ATR method is far less frequent. Broader, less symmetric, reflectivity curves leads to the experimental data being recorded over much larger angle ranges, see Fig. 9, after Innes and Sambles [31]. This can cause detection problems, as mentioned previously. As the incident wavelength is reduced so interband contributions become more important, increasing the films absorption, and thus predominately the imaginary part of the dielectric constant, which broadens the half-width of the reflectivity resonance. At 425 nm, curve (a) in Fig. 9, the amount of reflected light is very much reduced and the reflectivity resonance is a broad featureless curve. Obtaining accurate experimental data at these short wavelengths is vital for the correct determination of the dielectric function. Because of the very wide angle range that

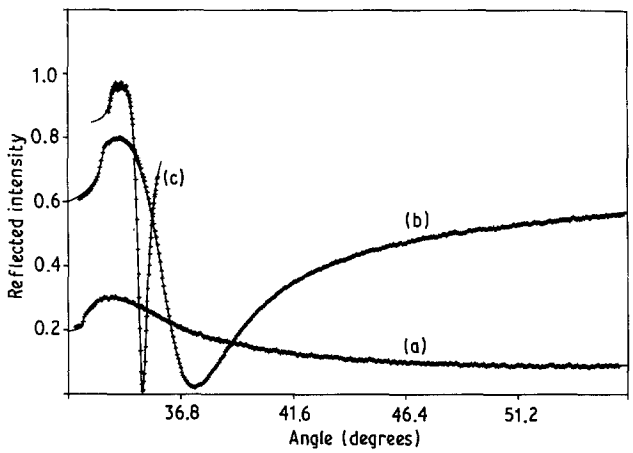

Figure 9 Reflected intensity as a function of angle of incidence showing SPP excited on a gold film at three wavelengths (a) 425 nm, (b) 550 nm, and (c) 700 nm. Experimental data, (+++) are well predicted by theory, (——) after Innes and Sambles [31].

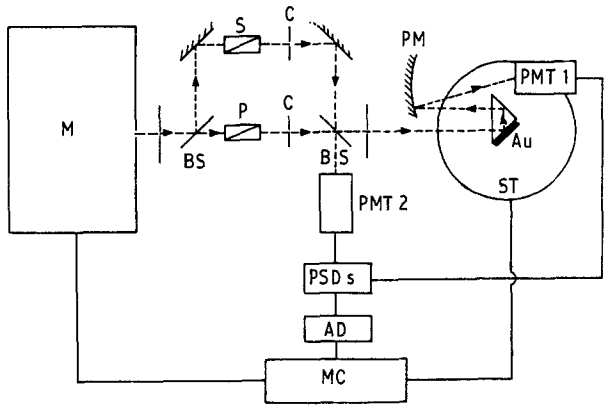

Figure 10 Modification of ATR angle scanned SPP excitation with monochromated, *M*, light source suitable for wide angle scans. Use of the parabolic mirror, PM, allows reflectivity versus angle scans to be monitored by a stationary detector, PMT1. *P*- and *S*-polarised beams are recombined by beam splitter, BS and amplitude modulated by choppers, C, and then detected via phase sensitive detection, PSD, and A/D converters by a microcomputer, MC, which controls the rotation of the spectrometer table, ST, after Innes and Sambles [31].

has to be recorded, care in the detection system has to be taken and the approximate double angle technique used by Gugger *et al.* is no longer suitable. Innes and Sambles employ a somewhat more elegant experimental system in which the gold thin film is evaporated on to one face of a retroreflector prism. The incident light beam is composed of both a *p*-polarised beam and an *s*-polarised beam, modulated at different frequencies so that the *s*-beam can be used as a monitor of variation in detector response *etc.* As the retroreflector is rotated the reflected beam is always parallel to the incident beam and is directed towards a parabolic mirror (PM) which reflects the beam to its focus, see Fig. 10. Thus for all prism rotation angles the reflected beam passes through the mirror focus at which a stationary detector is placed.

Perturbations of the SPP ATR reflectivity response caused by the close proximity, or contact, of dielectric media allows information to be gained about the properties of the dielectric in the interfacial region.

5. Dielectric properties of inorganic overlayers

We have already seen how the electromagnetic fields associated with the propagating SPP extend only a short distance into the dielectric half-space adjacent to the surface active medium. Alterations in this dielectric environment perturb the fields, which modifies the propagating surface wave, and consequently are observed as modifications to the reflectivity response of the system. Because these electromagnetic fields decay, typically over a distance of one wavelength, perpendicular to the interface, it is alterations to the dielectric properties in this region that dominate modifications to the reflectivity response. SPPs are thus highly sensitive thin film monitors.

Although a full analysis of the reflectivity response using Fresnel's equations is most often required to extract the thickness and the optical constants of the overlayer there are general characteristic modifications to the reflectivity response which identify either lossless or lossy overlayers. The standard work demonstrating these effects is due to Pockrand [32]. Studying the effect of depositing progressively thicker layers of the lossless dielectric

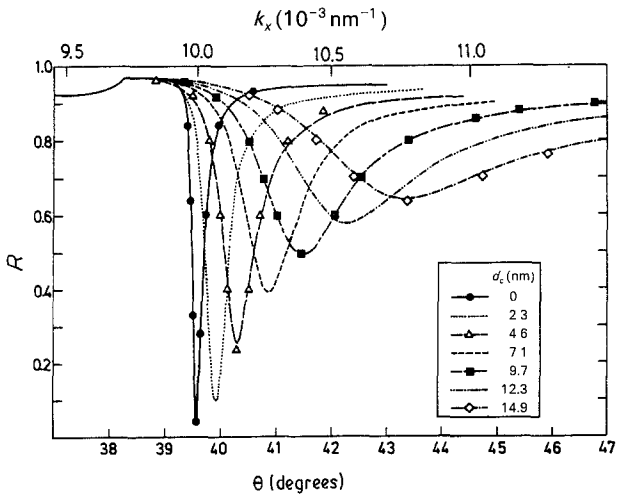

Figure 11 Experimental SPP resonance curves for a silver film showing the effect of various thickness overlayers, d_c(nm), of the lossy material carbon. Continuous lines are experimental data and symbols mark least squares fitted theory, after Pockrand [32].

lithium fluoride (LiF) on to a silver surface, in the Kretschmann–Raether geometry, Pockrand was able to predict that the wavevector of the SPP would increase. This is as expected since the electromagnetic fields in the dielectric half space are made to propagate through progressively more of a denser dielectric, thus slowing the wave and increasing the wavevector. In a reflectivity versus angle representation, the angle of incidence for optimum excitation of the surface wave increases. Increasing the thickness of the lossless dielectric modifies the distribution of energy propagation in the layered structure. Electromagnetic fields in the dielectric region are collapsed toward the interface, as the higher density film increases in thickness, and results in more energy being transported by the metal film. Although the fields in the dielectric region experience no loss due to the overlayer the larger proportion of energy propagating in the metal layer causes the SPP to experience increased damping and thus the half width of the reflectivity resonance increases as the lossless film thickness grows. Because optimum coupling occurs when the Joule heating losses in the metal match the radiation losses back into the prism, and Pockrand was able to show that these two losses remain matched, no change in the reflectivity minimum depth is expected. Experimental verification of these predictions have been provided by Pockrand. For lossy dielectric films the effect on the reflectivity response is somewhat different. Depositing the more dense medium on to the surface active medium again increases the surface wave vector, thus increasing the incident angle for optimum coupling. As before, the electromagnetic fields will be confined more strongly to the metal interface by the thin film layer, thus increasing the proportion of the energy propagated in the metal layer. Damping of the SPP again increases but at a much greater rate since energy is being lost not only in the metal but also in the thin film. Although radiative losses also increase they cannot now compensate for the enhanced material losses and optimum coupling is progressively lost as the film thickness increases. Pockrand was able to illustrate his predictions by experimentally investigating thin carbon film deposition, Fig. 11. Here we notice that the depth of the reflectivity minimum rapidly decreases with carbon film thickness, whereas the optimum

coupling angle and the half width of the reflectivity resonance increase. Besides inorganic overlayers, organic systems can also be examined using the SPP.

6. Analysis of systems involving organics

Systems involving organics can be broken down into three main categories. Firstly, there are those in which the organic material may be treated as an isotropic thin film or bulk layer, such as inorganic fluid condensation on metal surfaces. Studies of organic, isotropic, fluids have been conducted by Sambles *et al.* [33] and Pollard *et al.* [34], the details of which can be found in the literature. Secondly, there are those in which the organic material behaves uniaxially birefringent where a more complete description of the system relies on bulk guided wave analysis, such as in liquid crystal layers.

Any modifications in the liquid crystal surface director orientation with voltage can be sensitively probed using the SPP. First to study liquid crystals using a SPP were Swalen and Sprokel [35]. Later studies by Sprokel *et al.* [36], and Sprokel [37], were able to provide a theoretical understanding of the experimental results. However, the predicted shifts in the position of the SPP reflectivity minimum were less than the experimental shifts for all applied voltages and the liquid crystal model they were incorporating was suggested to be inadequate. An explanation of their findings, and a more thorough investigation of a parallel aligned liquid crystal layer, has been provided recently by Welford and Sambles [38]. A striking difference between the experimental reflectivities of Sprokel *et al.*, which showed only a single reflectivity minimum, and those of Welford and Sambles, is that in the latter a large number of closely spaced resonances appear superimposed on the broader single resonance associated with the SPP see Fig. 12. Deforming the liquid crystal, with an applied voltage, gradually forms a graded index waveguide and each of the narrow reflectivity minima corresponds to allowed, phase matched, guided modes in the bulk of the liquid crystal. Calculations of the Poynting vector in this liquid crystal layer by Innes *et al.* [39] show that guided waves are indeed supported by the deformed director profile. In this work the SPP was able to accurately monitor surface effects while the guided waves

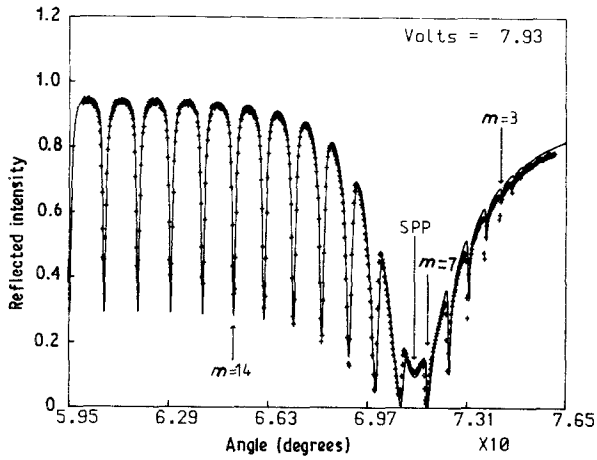

Figure 12 Reflectivity against incident angle for SPP on silver propagating in a nematic liquid crystal environment at 7.93 V. Marked are the minima associated with the SPP and various guided waves, after Innes *et al.* [39]. (+++), experimental; (——) theoretical.

monitored the bulk effects. The selectivity of the SPP helped throw new light on the surface reorientation effects in liquid crystals.

Currently, investigations of much more complicated smectic liquid crystal systems are being successfully probed using a combination of guided waves and SPP methods, see Elston *et al.* [40], and Elston and Sambles [41]. So far, however, the SPP is yet to contribute as strongly in the understanding of smectics as it has in nematic surface forces.

In addition, there is the most challenging case of biaxial materials which necessarily rely on information provided by bulk guided wave experiments to allow SPPs to probe down to the monolayer level, Pockrand *et al.* [42]. Examples of such systems are Langmuir–Blodgett (LB) films. Using both guided waves and SPPs, Barnes and Sambles [43, 44] have recently presented results showing how LB films begin growing on hydrophillic and hydrophobic substrates.

If LB films are deposited, incorporating molecules exhibiting an absorption band, SPP can be used to gain information about the dispersion of monolayers of material, see Pockrand and Swalen [45]. In general complete analysis relies upon experimental analysis of thick LB layers with guided waves, as well as the monolayer samples.

7. Coupled surface plasmon-polaritons

So far we have considered a single metal/dielectric interface supporting a SPP in two configurations. First, where the electromagnetic fields couple across a dielectric layer, the Otto configuration, and second, where coupling occurs across a metal layer, the Kretschmann–Raether configuration. Consider the Otto geometry in which the dielectric coupling gap is fixed and the thickness of the metal layer is reduced so that the second metal surface comes into the proximity of the exponential fields. If the coupling layer and metal thicknesses are chosen correctly both the Otto and Kretschmann–Raether excitation may be excited, simultaneously, in one system. One of the first experimental studies of coupled SPPs was performed by Kovacs and Scott [46]. Coupling of the two surface charge distributions results in two possible coupled surface waves. Either the surface charges on the two metal surfaces oscillate symmetrically, so that negative charge regions on one surface coincide with negative charge regions on the second metal surface, forming a high momentum mode, or the oscillating surface charges couple antisymmetrically, forming a lower momentum surface mode. Altering the refractive index of the dielectric layer by as little as 3% results in a decoupling of the two modes, even though the coupling angles are only slightly modified. Two ingredients are therefore essential to excite coupled surface plasmons. Firstly, the metal/dielectric interfaces must be sufficiently close for the electromagnetic fields to interact, and that the dielectric environments of the interfaces must be closely matched. Because of the way in which the surface charge density oscillations couple, the symmetric mode preferentially excludes the electromagnetic fields from the metal, whereas the antisymmetric mode partly enhances them. Consequently the Joule heating loss is less in the symmetric mode, which increases the propagation length of this mode. The symmetric, larger wave vector, mode is referred to as the long range surface plasmon (LRSP) and the antisymmetric mode, the short range surface plasmon (SRSP). Not only is the propagation distance in this mode enhanced so too are the surface field enhancements. Interest in this mode has focused on its potential applications in non-linear optics. Many authors have made experimental investigations of the propagation constants of SPPs on thin metal films, with varying levels of success. Control of film thickness and surface roughness, especially the problem of producing planar films with thicknesses $\approx 10\,\text{nm}$, have been central to the

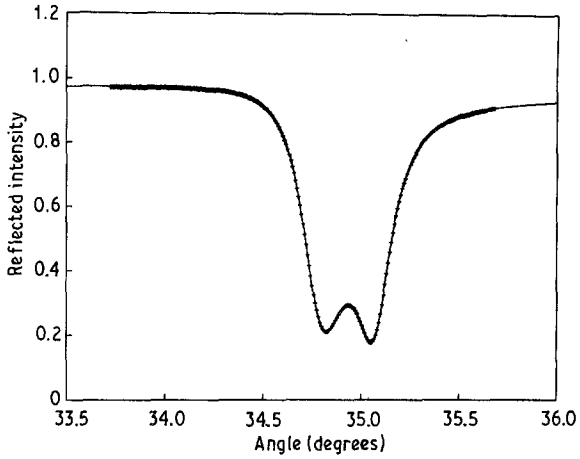

Figure 13 Reflectivity against incident angle showing the excitation of coupled SPP when the dielectric spacing between two silver layers is thin enough to allow excitation of both silver surfaces. Experimental data, (+++) is accurately predicted by theory only if non-parallel interface effects are modelled after Welford and Sambles [50].

experimental difficulties. Sharp reflectivity minima with FWHM ≈ 1 mrad have been achieved by Craig *et al.* [47] using metal films ≈ 10 nm.

In most experimental studies, the dielectric constants of the materials adjacent to the thin metal layer have been matched. This is necessary for the excitation of coupled SPP. However, the dielectric environments of each metal/dielectric interface is only pseudo-symmetric because of the presence of the glass coupling prism on only one side. If a fully symmetric system is constructed, transmitted light can be monitored, see Dragila *et al.* [48]. When the incident light angle is chosen to match the optimum coupling angle for a coupled SPP, the reflected intensity falls to zero at the same time as the transmission reaches 70%, provided the coupling gap thickness is chosen correctly.

Consider the alternative arrangement for exciting coupled SPPs between two metal/dielectric interfaces separated by a dielectric layer, and not a metal layer. As before, to generate coupled SPPs the distance between the two interfaces has to be small and the dielectric constants either side of both interfaces must match. Investigations of this type of structure, using MgF_2 and silver layers, by Kovacs and Scott [49], established this alternative arrangement. In this, and many subsequent experiments, the interface roughness limits the usefulness of the data. In recent work, by Welford and Sambles [50], this shortcoming has been overcome by using air spacing between the two metal interfaces. In addition, by investigating a fully symmetric system, the transmission properties can be examined. Thin silver films are evaporated onto two glass prisms and the two silver interfaces brought close together to trap a thin air layer between them. Adjusting the thickness of this air layer allows the degree of coupling between the two metal interfaces to be continually variable. When the air layer is wide, 2.80 μm, only the single interface Kretschmann–Raether mode is excited along with guided waves trapped between the two metal interfaces. If the air layer is reduced in thickness, the coupling between the single interface SPP and the second silver interface, is enhanced. Initially, the transmitted energy increases before the single reflectivity minimum splits into two minima, one at higher coupling angles and one at lower coupling angles. These correspond to the symmetric and antisymmetric modes respectively, see Fig. 13.

As far as is known this is the first demonstration of the transformation of a Kretschmann–Raether mode into a coupled SPP. Reducing the air layer thickness increases the interaction between the two metal interfaces, causing the LRSP mode to move to progressively longer wave vectors and the SRSP mode to shorter wave vectors. Discussion of more complicated systems, with three dielectric layers and a thin metal layer, by Kou and Tamir [51], demonstrates the way in which the surrounding dielectric environment can be fashioned to extend the range of coupled SPPs. Devices utilizing electro-optic dielectrics to modify the SPP coupling condition have been proposed as electro-optic modulators for some years, see Sincerbox and Gordon [52], but recently the narrower FWHM achievable with coupled SPPs has been proposed as an improvement of the basic SPP electro-optic modulator by Schildkraut [53]. High reflection, high contrast devices incorporating an organic electro-optic layer appear to show great promise.

A recent, and important, development in coupled surface polaritons has been given by Yang *et al.* [54]. They have been able to demonstrate a previously undiscovered long range surface exiton polariton (LRSEP). Basically, a highly lossy vanadium oxide layer, 45 nm thick, has been used to support a long range surface polariton. This mode is not a plasmon mode, since the active medium does not show a negative permittivity. The number of materials that are now available for supporting coupled polaritons is extremely wide. Applications of this new polariton mode are numerous and it will be interesting to follow future developments.

8. Application of enhancement effects

Previous discussions have shown that at resonance the SPP provides enhanced electric fields at the metal interface and also enhanced absorption of energy, which through Joule loss, can provide strong heating at the interface. These two aspects have found applications in both linear optics, with improved measurement sensitivity in a host of experiments, and non-linear optics, enhancing both second order and third order effects.

8.1. Linear Pockels effect

Langmuir–Bodgett (LB) films have shown potential in electro-optics through second harmonic generation and both the Stark effect and the Pockels effect. First to measure the Pockels effect, in an LB film, were Cross *et al.* [55] using a SPP measurement to monitor very small changes in the dielectric constant of the material, when placed in an electric field. A conventional Kretschmann–Raether configuration was constructed with a single monolayer of the LB material deposited onto the silver interface. To provide an electric field across the organic layer, without damaging it, a top electrode of ITO, on a glass substrate, was brought within 6 μm of the surface, spaced by insulating material. Applying an electric field causes an alteration of the monolayer's dielectric constant, through the Pockels effect. Because this modifies the dielectric environment of the silver interface, the SPP propagation constant is affected and hence the minimum in the reflectivity response of the system moves to a slightly different angle. However, with a single monolayer refractive index changes as small as 10^{-5} need to be detected. Such small refractive index changes only slightly modify the reflectivity response and recording an accurate change in reflectivity, ΔR, as a function of incident angle is not possible. Overcoming this problem Cross *et al.* improved the sensitivity of their SPP experiment by modulating the applied voltage and detecting the differential reflectivity, at this modulation frequency. An extension of this preliminary work, by Loulergue *et al.* [56] studied the Pockels effect in centrosymmetric and noncentrosymmetric LB multilayers as the film thickness was altered.

8.2. Second harmonic generation

Soon after the method of ATR excitation of SPPs was demonstrated the idea of utilising the strong interfacial field enhancement to create second harmonic generation (SHG) at a silver surface was investigated by Simon *et al.* [57]. In their experiment the conventional single interface SPP, in the Kretschmann–Raether configuration, was excited and the SHG was monitored in reflection. Rather than using the surface active medium directly as the source of non-linear polarisation, the SPP electric field enhancement is more usually used to enhance the SHG of a non-linear dielectric adjacent to the metal interface. Simon *et al.* [58] experimentally demonstrated enhanced SHG, in quartz adjacent to a single interface SPP, with an enhancement factor of some 50 times. A theoretical study of the SHG enhancement in quartz, adjacent to a single interface SPP in the Kretschmann–Raether geometry, compared with the enhancement possible if the LRSP is used as an alternative, was performed by Deck and Sarid [59]. This work demonstrated that if the metal thickness is chosen correctly and the dielectric constant of the spacer layer is matched to that of the quartz, the LRSP mode could be excited, with an enhancement of the SHG of 300 times over that of the conventional Kretschmann–Raether mode. Of course, the LRSP is not the only mode that can be excited in this type of geometry, although it is by far the most strongly enhanced. Slightly modifying the thickness of the coupling layer the SRSP(ω) can be excited resulting in enhanced SHG, but not as strong as in the LRSP(ω) case. Satisfying the coupling conditions for the frequency doubled coupled-SPP leads to SHG also, but at much lower enhancements. Experimental verification of these predicted effects was first achieved by Quail *et al.* [60]. In their experimental geometry a thin film of silver was evaporated onto the quartz crystal surface and coupled to the prism by an index matched fluid. They were able to show that the reflected SHG light increased by over four orders of magnitude as the LRSP(ω) was brought into optimum excitation. An ingenious experiment by Quail and Simon [61] demonstrated how phase matching the SRSP(ω) mode with the LRSP(2ω) mode can lead to still further improvements in the SHG in quartz. Besides these single input beam experiments other more novel approaches to SHG have been investigated, like the mixing of two counterpropagating LRSPs studied by Stegeman *et al.* [62].

8.3. Intensity dependent refractive index

One of the most fascinating effects possible with a material exhibiting a non-linear refractive index is optical bistability (OB). Optical bistability essentially relies on two factors, optical feedback, and field enhancement. Optical feedback, in the SPP geometry, occurs since the reflectivity at a particular angle depends on the refractive index adjacent to the surface active medium, which depends on the intensity of the SPP, which in turn depends on the reflectivity of the system, thus a positive feedback is established. Theoretically first proposed by Wysin *et al.* [63], using the conventional single interface Kretschmann–Raether SPP at a silver/CS_2 boundary, an order of magnitude reduction in the critical switching intensity was predicted over previously discussed OB at a single interface. Hickernell and Sarid [64] compared the switching intensities for a single interface SPP and a coupled LRSP and demonstrated that a further reduction in switching intensity of two orders of magnitude can be achieved. A more intuitive approach to understanding the OB was proposed by Martinot *et al.* [65] using a graphical approach, similar to that often used in the explanation of OB in Fabry–Perot resonators. They note that to prevent CS_2 attacking the silver surface, a dielectric coating must be placed on the silver. So that the coating does not affect the

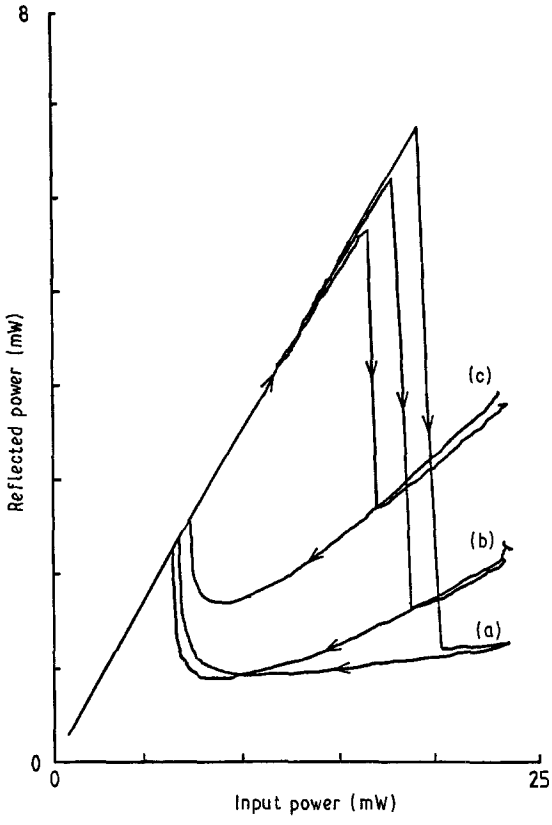

Figure 14 Reflected power as a function of incident power (spot size $3 \times 10^{-4}\,cm^2$) at angles of incidence (a) 71.02°, (b) 72.08°, and (c) 73.3° after Innes *et al.* [69] in a liquid crystal system.

propagation of the SPP, they propose that the silver film is evaporated onto a linear substrate, with a protective SiO_2 coating on, and is brought into contact with the CS_2 through which the incident light is directed. Since the SPP is excited at the metal/linear dielectric interface, the field enhancements within the CS_2 are not expected to be dramatic. Nonetheless they were able to demonstrate, theoretically, bistability in the $10\,GW\,cm^{-2}$ range. However, as expected, this is much greater than $0.5\,GW\,cm^{-2}$ predicted by Wysin *et al.* Interestingly, the experimental study of this system by Martinot *et al.* [66] was not analysed in terms of their previously proposed electric field dependent refractive index, via a third order non-linearity, but in terms of thermal non-linearity, again using a graphical approach. Using the conventional meaning of critical switching Martinot *et al.* [66] were able to show a critical intensity as low as $2\,KW\,cm^{-2}$ with a switching time $\approx 100\,ms$. Consideration of thermal effects, in experiments which attempt to access enhanced non-linearities due to field enhancements, have been discussed recently by Sambles and Innes [67]. They point out that thermal effects, in thin metal film geometries, always dominate field enhancement effects and suggest that the only geometry likely to exhibit field dominance is the Otto geometry, where the bulk of the metal film can be used as a heat sink. By suitably orientating a liquid crystal adjacent to a SPP supporting metal surface, strong non-linear effects can be demonstrated, Innes and Sambles [68] and Innes *et al.* [69], see Fig. 14. Since the thermal non-linearity accessed here is due to the change in refractive index induced in heating the liquid crystal across the nematic to isotropic phase transition, the response time of the effect was determined to be in the 10 ms range.

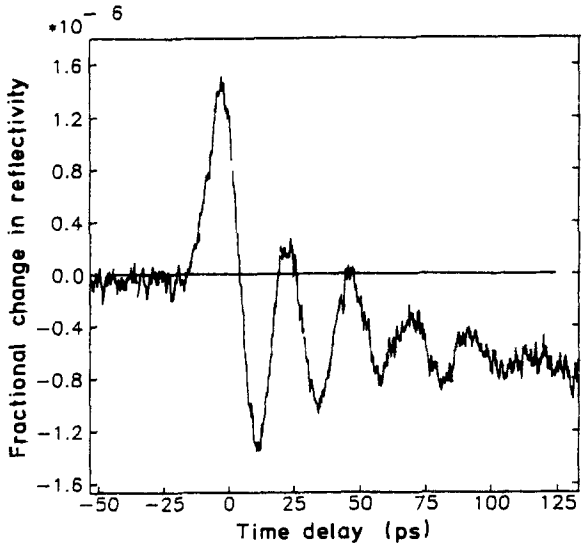

Figure 15 Detail of the short time-decay of the reflectivity. Oscillations are due to acoustic phonons in the silver film with a period of 23.8 ps. Amplitude decay is due to acoustic reflection at the glass–silver interface, after Van Exter and Lagendijk [70].

9. Time resolved studies

Recently the study of the physics of SPP has been extended to investigate their temporal response using optical pulse-probe methods.

The pioneering work by Van Exter and Lagendijk [70] utilized two mode locked dye lasers, producing 5 ps pulses, to indirectly determine the lifetime of the SPP. Both lasers, operating at slightly different wavelengths, were colinearly incident at the SPP excitation angle. Arrival of the pump beam causes the excitation of a SPP, which then decays via Joule heating of the metal film. Heating of the film, which is proportional to the field strengths induced by the SPP, causes minute changes in the dielectric constant of the metal film, in this case silver, and thus minor changes in the reflected intensity of the probe beam. Relative reflectivity changes in the probe beam $\approx 10^{-4}$ are then induced by the small change in the temperature of the metal film, estimated to be 1 K. Delaying the probe beam by a fixed amount, a few tens of picoseconds, the reflectivity change can be spatially mapped by moving the probe with respect to the pulse. Analysis of their results lead them to conclude that the decay length of the SPP is $\approx 12.8\,\mu$m. Linking this with the theoretical group velocity of the SPP, they indirectly determine the lifetime to be 48 fs. Studying the temporal, as opposed to the spatial, properties of the reflectivity change they clearly demonstrate two distinct decay processes, one operating on the nanosecond timescale and the other on the picosecond time scale. When the pump beam arrives at the silver film it drives the free electrons to excite the SPP. As the oscillating charges decay they heat a very thin region of the silver film close to its surface creating acoustic phonons, which propagate away in all directions. Those propagating perpendicular to the surface are reflected from the silver/prism interface, arriving back at the surface region some time later, affecting the reflectivity of the silver film in a periodic fashion. This effect can be clearly seen in Fig. 15 after [70]. Knowing the thickness of the silver, from a quartz-crystal monitor measurement, Van Exter and Lagendijk calculate the phonon velocity to be $3.78\,\mathrm{km\,s^{-1}}$ from the period of the

reflectivity oscillation, which is in close agreement with the sound velocity in bulk silver. Decrease in the amplitude of the acoustic signal is accurately predicted by the reflection coefficient of acoustic phonons at the silver–glass interface being $\approx 50\%$. After the silver film has been heated by the decaying SPP the relaxation of the change in reflectivity is determined by the heat diffusion rate away from the excitation position. Due to the film thinness this is dominated by heat diffusion into the prism material. Recovery of the equilibrium temperature was measured to be over many nanoseconds. This work has been further extended to study electron–phonon relaxation in silver by Groenveld *et al.* [71].

A more direct determination of the decay times of SPP on grating surfaces was conducted by Kroo and Szentirmay [72]. For a given periodicity of the grating the amplitude determines the decay time of the SPP. Increasing the amplitude of the grating reduces the life time dramatically. If the periodicity is due to several Fourier components, the reduction in the SPP lifetime is further enhanced. Studying electron-micrographs of their gratings, Kroo and Szentirmay showed that more than one wavelength was evident and they model their grating profile using four Fourier components. This affected the SPP lifetime by up to 50%. When comparison between experiment and theory was made it showed that the experimental results were within 10% of their predictions. With a grating amplitude of 16.4 nm the experimental lifetime was measured to be 66 fs, whereas with the amplitude increased to 44.4 nm the lifetime fell to $\leqslant 10$ fs. Kroo and Szentirmay point out that the expected planar surface lifetime for SPP is 200 fs which disagrees with the 48 fs measured by Van Exter and Lagendijk.

This work opens up a whole new field of SPP study which could investigate SPP lifetimes as a function of excitation wavelength, grating parameters, temperature etc. allowing experimental checks to be made on well established theory.

10. Device application

Although SPPs have some unique and interesting properties these have so far been rarely applied to device fabrication. This situation appears to be slowly changing with the two currently most topical applications being in optical sensors and surface imaging.

10.1. Optical sensors

Early demonstrations using SPPs as optical gas detectors, Nylander *et al.* [73], and optical biosensors, Liedberg *et al.* [74] and Flanagan and Pantell [75], have recently been receiving much renewed attention with a view to improving on the basic principle of operation. Any alteration in the dielectric environment at the surface active medium leads to a modification in the SPP dispersion, thus resulting in a modification in the optical properties of the system. Monitoring the optical changes in the SPP induced by a change in the dielectric environment constitutes the basis of the optical sensor. As we have seen already, there are various experimental parameters which can be measured to quantify an alteration in the properties of the SPP.

By far the simplest is to record the change in the angle of minimum reflectivity, $\Delta\theta_{spp}$, and it is this parameter that was monitored in each of the early studies. Enhancement of the sensitivity of the SPP to small quantities of a gas in the environment adjacent to the surface active medium is achieved by coating the metal surface with a thin film material which preferentially absorbs the gas species to be monitored. Trapping the gas molecules within the film, often via a chemical reaction, results in a small change in the refractive index of the thin film, proportional to the concentration of the gas molecules, which results in a

measureable change in the optimum coupling angle for SPP excitation. Using a 43 nm thick film of a silicon–glycol copolymer, deposited on a metal layer, Liedberg *et al.* were able to rapidly, and reversibly, record the concentration of halothane down to 100 ppm. To achieve this angle changes as small as 0.002° need to be measured. Two shortcomings of this device are immediately apparent. Firstly, the selectivity of the silicon–glycol copolymer is relatively poor. Although the sensitivity is < 100 ppm, the detected species could be any halogenated hydrocarbon, not just halothane. And secondly, although the SPP is highly sensitive to variations in the dielectric environment, and as such makes an ideal transducer, recording $\Delta\theta_{spp}$ is exacting and complicated. Major contribution in recent years has come more from addressing the experimentation of detecting changes rather than from chemical selectivity. Perhaps more rewarding model systems to investigate are the inherently more selective antigen–antibody reactions. First investigated by Nylander *et al.*, Liedberg *et al.* and Flanagan and Pantel, and more recently by Daniels *et al.* [76] these biosensors are rather different to the gas sensors in several aspects. Although they are more selective their speed of response is slowed to many minutes and a non equilibrium situation is created. This results in the reflectivity resonance not reaching a steady state. However, the initial rate of change of SPP resonance angle is directly proportional to the antigen concentration, so that within a few seconds the concentration can be determined. In more recent work, Daniel *et al.* worked at fixed angle and monitored the change in reflectivity. Choosing the operating angle to be where the maximum rate of change of reflectivity occurs, that is, at roughly the FWHM point, small changes in the SPP resonance angle generate significant modifications of the reflectivity. Working wholely in terms of ΔR and dR/dt, Daniels *et al.* were able to measure antigen concentrations to the nanomolar level. Although far more selective than the active layers in current gas sensors, antibody layers are not, in fact, uniquely selective, see Liedberg *et al.* [74].

Although working with the reflectivity is a major step forward, compared to monitoring the alteration in resonance angle, it suffers from two new problems. Firstly, an alterations in the incident light intensity appears as a reflectivity alteration, unless a reference beam is monitored simultaneously and, secondly, large changes in the dielectric environment become difficult to handle since the reflectivity can fall to zero, and even move in the opposite sense as the resonance angle shifts past the chosen fixed monitoring angle. A new approach which appears to combine the fixed angle attribute with the recording of a minimum, thus eliminating the problems just mentioned, has been introduced recently by France and Jones [77] and Zhang and Uttamchandani [78]. In their work they have used a white light input and monitored the change in the wavelength showing minimum reflectivity.

Rather than fixing the incident angle of the beam inside a conventional prism arrangement, Stewart *et al.* [79] have taken a further step towards a more integrated device by theoretically, and experimentally, investigating the coupling between a mode guided in a fibre optic and a SPP excited on a thin metal film, coating the fibre. Polishing the outer cladding, to reduce its thickness, a flat is fabricated on the fibre optic wall onto which a thin metal layer is evaporated. If the thickness is chosen correctly, coupling can be achieved between a guided mode and the SPP, for a given overcoating refractive index. An extinction ratio between the TE and TM excitations of -50 dB can be achieved. Clearly this has applications as a polariser, but recording variations in the extinction ratio may lead to an optical sensor application. Polarising beam splitters [80] and polarising couplers [81, 82] are further fibre/SPP devices currently receiving attention in the literature.

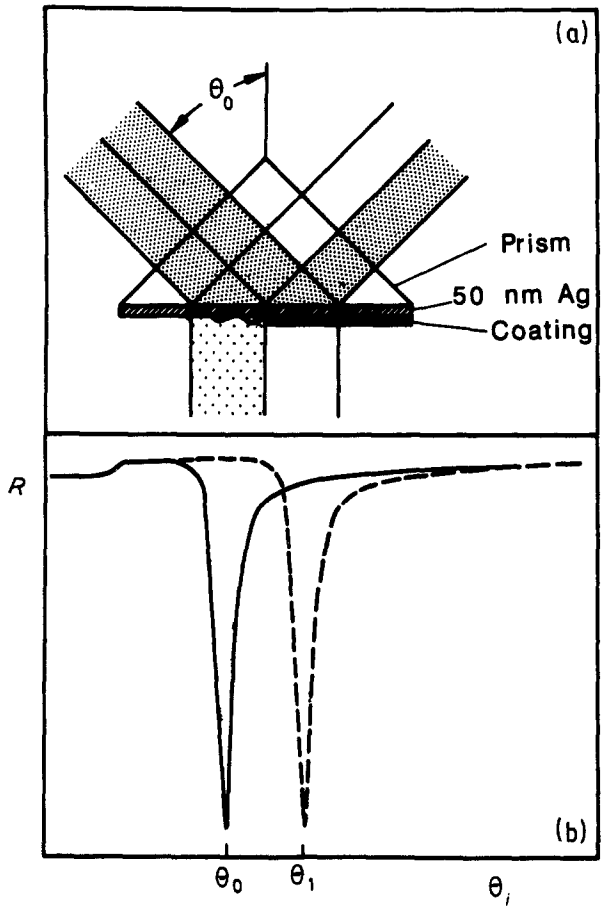

Figure 16 (a) Schematic illustration of the contrast mechanism in SPM. Half the silver film is covered by a thin coating which shifts the SPP resonance angle. At θ_0 only in the uncoated region are SPP excited. Some light is roughness coupled into the air. The coated region is off resonance so total reflection occurs. (b) Reflectivity, R, against angle of incidence, θ_i, for coated, (– – –) and uncoated, (——) regions, after Rothenhausler and Knoll [85], (Copyright © 1988 Macmillian Magazines Ltd).

10.2. Surface imaging

In all of the previous studies of a layered structure using a SPP a parallel, approximately plane wave, incident beam has been the input light. Recording the reflectivity, point by point, as the incident angle is varied, the ATR spectrum is gradually built up. Each experimental reflectivity measurement is an indication of the coupling strength to the SPP, for a single **k** vector, averaged over the area of the beam. Surface imaging using SPPs is concerned with either mapping a region of **k**-space at a given spatial position or mapping the spatial dielectric variations with either a focused, scanning, incident beam or a collimated, stationary beam using a microscope arrangement. These latter two approaches are variations of the surface plasmon microscope (SPM). Presently, imaging methods have concentrated on the real space image of the surface by Fourier back transforming the reflected light with an output lens. Pioneering studies were initiated by Yeatman and Ash [83] and Rothenhausler *et al.* [84]. A plane wave is incident through a prism onto the metal film

which is coated with the layer to be analysed. Choosing the incident angle to be θ_0, the SPP is excited in an uncoated region, reducing the reflected intensity to near zero, but the reflected intensity remains high in the coated region. This is pictured schematically in Fig. 16. Imaging the reflected beam with a lens creates a high contrast image of the area sampled by the incident beam, showing coated regions as dark on a light background. The two important considerations for any microscopy are contrast and lateral resolution. For imaging very thin layers, even single monolayers of transparent organic material, the SPM is unsurpassed [85]. We can see that the minimum thickness of the layer that allows full constrast is achieved when $2(\theta_1 - \theta_0) \approx$ FWHM. This condition is reached for layers of nanometer thickness. If instead of fixing the incident angle at θ_0 it is altered to θ_1 the contrast is reversed since now the SPP is excited in the coated region only. Increasing the thickness of the layer does not enhance the contrast of the image. All that happens is that θ_1 will increase but the reflectivity difference between the solid and dashed curve in Fig. 16 will remain the same. Lateral resolution is primarily determined by the propagation distance of the SPP, which is typically $\approx 25\,\mu$m. An attempt to improve this limit by Yeatman and Ash [86] by using a focused incident beam was unsuccessful for a variety of reasons. Two major disadvantages are that the spread in incident angles leads to a broadening of the reflectivity minimum and hence a loss of sensitivity and contrast, and secondly the image of the surface has to be built up by scanning the incident light spot in a time consuming, mechanically complex, manner. Further developments in this area are on going, Hickel *et al.* [87], Hickel and Knoll [88] and Rabe [88].

11. Other types of surface polaritons

Briefly to finish, it is important to reiterate that SPPs are not the only form of surface polaritons. Other materials besides metals can support surface electromagnetic waves, such as semiconductors, organic and inorganic dielectrics. Of primary importance is that the dielectric function is negative. (As mentioned in the section on coupled polaritons, Yang *et al.* [54] have established the LRSEP, in a double interface system, that exists without the condition holding.) If this is achieved then a surface polariton can be generated in this wavelength region. For a recent review on surface polaritons in semiconductors and multiple quantum wells see Tilley [90] and the references therein. Also see El-Gohary *et al.* [91]. Materials as diverse as ZnSe [92], and more recently BeO [93], PTFE [94], and even high temperature superconductor material $YBa_2Cu_3O_6$ [95] exhibit surface polaritons in the ultraviolet and infrared. Substantial interest exists in SPPs in the infrared, and in infrared materials, mainly for spectroscopic purposes but also for possible infrared signal processing, Steijn *et al.* [96]. In the work by Steijn *et al.*, SPPs at a wavelength of 0.119 mm were studied propagating across a silver film, coated with an overlayer of silicon. Although propagation of many centimetres can be achieved in the infrared, the localisation of the bound mode to the surface is relatively weak, with fields extending up to 10^3 wavelengths from the interface. Steijn *et al.* used a thin coating of silicon to collapse the fields closer to the interface, at the expense of an increase in damping. Interestingly, they showed that the Drude free electron model for the dielectric permittivity is still valid at these long wavelengths. Because propagation distances are macroscopic, the SPP interacts with a large number of surface coating molecules – making it a sensitive spectroscopic tool. For a review of prism coupled spectroscopic methods see Alexander *et al.* [97]. Applications of SPP to Raman spectroscopy is becoming particularly prevalent at the present time, as a route to examining vibrational modes in monolayer organic films. Original work by Knoll *et al.* [98] is currently being

refined by Duschl and Knoll [99], and more recently by Knobloch *et al.* [100]. In addition, the surface enhanced Raman scattering (SERS) technique owes its sensitivity, in part, to field enhancements by SPP excitation, [101]. A further adaptation of the use of SPP in infrared spectroscopy is due to Silin *et al.* [102], in which they are concerned with investigating surface states using absorption and phase spectroscopy, simultaneously. Interest in infrared, 10.6 μm, modulators based on semiconducting materials, GaAs technology, is emerging, due to the work of Kuijk and Vounckx [103]. An area associated with the SPP propagating finite distances along interfaces is that of SPP optics, see Stegeman *et al.* [104]. Here the effect on a SPP of encountering a change in the dielectric environment during its propagation path, due to an edge of an overlayer, for instance, is considered. This work has applications in spectroscopy, perhaps, and also as a route to an alternative excitation method for SPP, by propagating a wave from a 'launching' environment into an 'active' environment, with applications in non-linear SPP excitation. Again, non-linear SPP have not been discussed, but see Boardman and Twardowski [105].

Of particular interest is the work by Swalen and coworkers [106, 107] on organic dye crystals which show a strong absorption band in the visible. Provided the lifetime of the absorption state is not too short, the real part of the dielectric function may become negative on the high energy side of the resonant frequency, consistent with simple Drude–Lorentz theory. This allows surface polaritons to be excited directly on these materials in the visible. Swalen and coworkers were able to experimentally demonstrate surface polaritons on two different organic dye materials [108, 109] at a range of wavelengths in the visible. Largely unexplored are the potentials of surface magneto-plasmons, excitable on magnetic materials, for a review see Wallis *et al.* [110]. Just one of the exciting properties in these types of system are the non-reciprocal propagating constants of the surface wave. With the application of a magnetic field the surface wave shows different dispersion depending on its direction of travel.

12. Conclusions

Through the course of this review it is hoped that the diverse and unique properties of SPPs have been elucidated. It should be realised that SPPs are but a small branch of a broader field of surface polaritons and an attempt to make this point has been made by briefly mentioning some of the many systems capable of supporting surface polaritons.

Within the relatively confined field of SPP, this review has only covered a proportion of the field. Only little mention has been made of SPP on grating surfaces not because this is an area of insignificance, on the contrary, these are most interesting systems, but in the interest of conciseness. Geometric constraints imposed by bulky glass coupling prisms having to be constructed from materials of suitable refractive index can be a limitation. Such problems are immediately removed if the surface of the material is profiled to form a grating, see Raether [1], Ritchie *et al.* [111], and Hutley [112]. For applications to device technology this is clearly an approach that offers much promise. The really new and exciting work lies in the area of time resolved SPP. For the first time direct measurements can be made of SPP lifetimes, albeit with a relatively sophisticated laser system. So far only the preliminary studies have been completed, investigating uncoated metal surfaces. A whole range of further experiments will follow, probing the physics of SPPs on coated surfaces, with the possibility of a new surface spectroscopic tool emerging.

The scope for future developments is unlimited and hopefully this review will sufficiently excite some to begin their own contributions to the field.

Acknowledgements

My interest in SPP stems entirely from working with Roy Sambles in the Thin Film and Interface Physics Group, Exeter, UK, whom I should like to thank for his encouragement and comments during the preparation of this article. Thanks also go to the journals for allowing the use of previously published figures.

References

1. H. RAETHER, *Physics of Thin Films* **9** (1977) 145.
2. A. OTTO, *Z. Phys.* **216** (1968) 398 and *Phys. Stat. Solidi.* **26** (1968) 199.
3. E. KRETSCHMANN and H. RAETHER, *Z. Naturf.* **230** (1968) 2135.
4. T. TURBADAR, *Proc. Phys. Soc. (London)* **73** (1959) 40.
5. A. D. BOARDMAN (Ed), 'Electromagnetic Surface Modes', (Wiley, 1982).
6. V. M. AGRANOVICH and D. L. MILLS (Ed), 'Surface Polaritons', (North Holland, 1982).
7. H. RAETHER, 'Surface Plasmons on Smooth and Rough Surfaces and on Gratings,' (Springer–Verlag, 1988).
8. J. R. SAMBLES, *J. Phys. Chem. Solids* **50** (1988) 1.
9. N. J. HARRICK, 'Internal Reflection Spectroscopy', (Wiley, 1967).
10. T. HIRSCHFIELD, *Appl. Optics* **6** (1967) 715.
11. P. K. TIEN, *Rev. Mod. Phys.* **49** (1977) 361.
12. J. D. SWALEN, *J. Phys. Chem.* **83** (1979) 1438.
13. R. H. RITCHIE, *Phys. Rev.* **106** (1957) 874.
14. R. H. RITCHIE and H. B. EDRIDGE, *ibid.*, **126** (1962) 1935.
15. K. L. KLIEWER and R. FUCHS, *ibid.*, **144** (1966) 495.
16. *Idem*, *ibid.*, **153** (1967) 498.
17. E. BURSTEIN, A. HARSTEIN, J. SCHOENWALD, A. A. MARADUDIN, D. L. MILLS and R. F. WALLIS, 'Polaritons', (Pergamon, 1974), edited by E. Burstein and F. De Martini, p. 89.
18. M. CARDONA, *Am. J. Phys.* **39** (1971) 1277.
19. G. J. KOVACS, 'Electromagnetic Surface Modes' (Wiley, 1982), edited by A. D. Boardman, Ch. 4, p. 143.
20. K. R. WELFORD, 'IOP Short Meetings Series Number 9: Surface Plasmon-Polaritons' (1988) p. 25.
21. A. D. BOARDMAN, 'Electromagnetic Surface Modes', (Wiley, 1982), Ch. 1, p. 20.
22. U. FANO, *J. Opt. Soc. Am.* **31** (1974) 213.
23. P. HALEVI, 'Electromagnetic Surface Modes', (Wiley, 1982), edited by A. D. Boardman, Ch. 7.
24. R. A. INNES and J. R. SAMBLES, *Sol. State Commun.* **56** (1985) 493.
25. W. L. BARNES and J. R. SAMBLES, *ibid.*, **55** (1985) 921.
26. C. A. WARD, K. BHASIN, R. J. BELL, R. W. ALEXANDER and I. TYLER, *J. Chem. Phys.* **62** (1975) 1674, 4960.
27. F. ABELÈS, Electromagnetic Surface Excitations, (Springer–Verlag, 1986), edited by R. F. Wallis and G. I. Stegeman, p. 26.
28. R. T. HOLM and E. D. PALIK, *Critical Rev. in Sol. St. Phys.* **5** (1975) 397.
29. J. D. SWALEN, J. G. GORDON, M. R. PHILPOTT, A. BRILLANTE, I. POCKRAND and R. SANTO, *Am. J. Phys.* **48** (1980) 669.
30. H. GUGGER, M. JURICH, J. D. SWALEN and A. J. SIEVERS, *Phys. Rev. B* **30** (1984) 4189.
31. R. A. INNES and J. R. SAMBLES, *J. Phys. F: Met. Phys* **17** (1987) 277.
32. I. POCKRAND, *Surf. Sci.* **72** (1978) 577.
33. J. R. SAMBLES, J. D. POLLARD and G. W. BRADBERRY, *Opt. Comm.* **63** (1987) 298.
34. J. D. POLLARD and J. R. SAMBLES, *Opt. Comm.* **64** (1987) 529.
35. J. D. SWALEN and G. J. SPROKEL, *The Physics and Chemistry of Liquid Crystal Devices*, (Plenum, 1980), edited by G. J. Sprokel, p. 39.
36. G. J. SPROKEL, R. SANTO and J. D. SWALEN, *Mol. Cryst. Liq. Cryst.* **68** (1981) 29.
37. G. J. SPROKEL, *Mol. Cryst. Liq. Cryst.* **68** (1981) 39.
38. K. R. WELFORD and J. R. SAMBLES, *Appl. Phys. Lett.* **50** (1987) 871.
39. R. A. INNES, K. R. WELFORD and J. R. SAMBLES, *Liq. Cryst.* **2** (1987) 843.
40. S. J. ELSTON, J. R. SAMBLES and M. G. CLARK, *J. Mod. Opt.* **36** (1989) 1019.
41. S. J. ELSTON and J. R. SAMBLES, *Appl. Phys. Lett.* **55** (1989) 1621.
42. I. POCKRAND, J. D. SWALEN, J. G. GORDON II and M. R. PHILPOTT, *Surf. Sci.* **74** (1977) 237.
43. W. L. BARNES and J. R. SAMBLES, *Surf. Sci.* **177** (1986) 399.

44. *Idem, ibid.*, **183** (1987) 189.
45. I. POCKRAND and J. D. SWALEN, *J. Opt. Soc. Am.* **68** (1978) 1147.
46. G. J. KOVACS and G. D. SCOTT, *Can. J. Phys.* **56** (1978) 1235.
47. A. E. CRAIG, G. A. OLSON and D. SARID, *Opt. Lett.* **8** (1983) 380.
48. R. DRAGILA, B. LUTHER-DAVIES and S. VUKOVIC, *Phys. Rev. Lett.* **55** (1985) 1117.
49. G. J. KOVACS and G. D. SCOTT, *Appl. Optics* **17** (1978) 3314.
50. K. R. WELFORD and J. R. SAMBLES, *J. Mod. Opt.* **35** (1988) 1467.
51. F. Y. KOU and T. TAMIR, *Opt. Lett.* **12** (1987) 367.
52. G. T. SINCERBOX and J. C. GORDON II, *Appl. Optics* **20** (1981) 1491.
53. J. S. SCHILDKRAUT, *Appl. Optics* **27** (1988) 4587.
54. F. YANG, J. R. SAMBLES and G. W. BRADBERRY, *Phys. Rev. Lett.* **64** (1990) 559.
55. G. H. CROSS, I. R. GIRLING, I. R. PETERSON and N. A. CADE, *Elec. Lett.* **22** (1986) 1111.
56. J. C. LOULERGUE, M. DOMONT, Y. LEVY, P. ROBIN, J. P. POCHOLLE and M. PAPOCHON, *Thin Solid Films* **160** (1988) 39.
57. H. J. SIMON, D. E. MITCHELL and J. G. WATSON, *Phys. Rev. Lett.* **33** (1974) 153.
58. H. J. SIMON, R. E. BENNER and J. G. RAKO, *Opt. Comm.* **23** (1977) 245.
59. R. T. DECK and D. SARID, *Opt. Soc. Am.* **72** (1982) 1613.
60. J. C. QUAIL, J. G. RAKO, H. J. SIMON and R. T. DECK, *Phys. Rev. Lett.* **50** (1983) 1987.
61. J. C. QUAIL and H. J. SIMON, *J. Appl. Phys.* **56** (1984) 2589.
62. G. I. STEGEMAN, C. LIAO and C. KARAGULEFF, *Opt. Comm.* **46** (1983) 253.
63. G. M. WYSIN, H. J. SIMON and R. T. DECK, *Opt. Lett.* **6** (1981) 30.
64. R. K. HICKERNELL and D. SARID, *J. Opt. Soc. Am. B* **3** (1986) 105.
65. P. MARTINOT, S. LAVAL and A. KOSTER, *J. Phys.* **45** (1984) 597.
66. P. MARTINOT, A. KOSTER and S. LAVAL, *IEEE J. Quan. Elec.* **QE-21** (1988) 1140.
67. J. R. SAMBLES and R. A. INNES, *J. Mod. Optics* **35** (1988) 791.
68. R. A. INNES and J. R. SAMBLES, *Opt. Comm.* **64** (1987) 288.
69. R. A. INNES, S. A. ASHWORTH and J. R. SAMBLES, *Phys. Lett. A* **135** (1989) 357.
70. M. VAN EXTER and A. LAGENDIJK, *Phys. Rev. Lett.* **60** (1988) 49.
71. R. H. M. GROENEVELD, R. SPRIK and A. LAGENDIJK, *Phys. Rev. Lett.* **64** (1990) 784.
72. N. KROO and Z. SZENTIRMAY, *Hung. Acad. Sci.* KFKI-1988-18/E.
73. C. NYLANDER, B. LIEDBERG and T. LIND, *Sens and Actuators* **3** (1982) 79.
74. B. LIEDBERG, C. NYLANDER and I. LUNDSTORM, *Sens. and Actuators* **4** (1983) 299.
75. M. F. FLANAGAN and R. H. PANTELL, *Elec. Lett.* **20** (1984) 968.
76. P. B. DANIELS, J. K. DEACON, M. J. EDDOWES and D. G. PEDLEY, *Sens and Actuators* **15** (1988) 11.
77. C. M. FRANCE and B. E. JONES, *Conf. Proc. Optical Fibre Sensors Tech. Digest Series* **24** (1988) 234.
78. L. M. ZHANG and D. UTTAMCHANDANI, *Elec. Lett.* **24** (1988) 1469.
79. G. STEWART, W. JOHNSTONE, B. CULSHAW and T. HART, *Conf. Proc. Optical Fibres Sensors Tech. Digest Series* **2** (1988) 328.
80. M. N. ZERAS, S. MARKATOS and I. P. GILES, *IEE Coll on all Fibre devices Digest* **90** (1988) 1.
81. W. JOHNSTONE, G. STEWART, B. ALLSHAW and T. HART, *Elec. Lett.* **24** (1988) 866.
82. M. N. ZERVAS and I. P. GILES, *Elec. Lett.* **25** (1989) 321.
83. E. YEATMAN and E. ASH, *Elec. Lett.* **23** (1987) 1091.
84. B. ROTHENHAUSLER, C. DUSCHL and W. KNOLL, *Thin Solid films* **159** (1988) 323.
85. B. ROTHENHAUSLER and W. KNOLL, *Nature* **332** (1988) 615.
86. E. YEATMAN and E. ASH, *SPIE* **897** (1988) 100.
87. W. HICKEL, B. ROTHENHAUSLER and W. KNOLL, *J. Appl. Phys.* **66** (1989) 4832.
88. W. HICKEL and W. KNOLL, *Acta. Metall.* **37** (1989) 2141.
89. J. R. RABE, *Advanced Materials* **2** (1990) 100.
90. D. R. TILLEY, *IOP Short Meetings Series number 9: Surface Plasmon-Polaritons*, (1988) 1.
91. A. R. EL-GOHARY, T. J. PARKER, N. RAJ, D. R. TILLEY, P. J. DOBSON, D. HILTON and C. T. R. FOX, *Semicond. Sci. Technology* **4** (1989) 388.
92. Y. TOKURA, I. HIRABAYASHI and T. KODA, *J. Phys. Soc. Japan* **42** (1977) 1071.
93. Y. A. BYKOVSKII, N. I. LIPATOV, S. P. MAKERENKO, Y. N. POLIVANOV and G. A. PUCHKOVSKAYA, *Sov. J. Quan. Elec.* **18** (1980) 220.
94. N. I. AFANASIEVA, E. G. BRAME Jnr, M. B. EZERNITSKAYA, B. V. LOKSHIN, V. A. YAKOVLEV and G. N. ZHIZHIN, *Polymer* **29** (1988) 821.

95. G. N. ZHIZHIN, K. V. KRAISKAYA, L. A. KUZIK, F. A. UVAROV and V. A. YAKOVIEV, *Sov. Phys. Solid State* **30** (1988) 541.
96. K. W. STEIJN, R. J. SEYMOUR and G. I. STEGEMAN, *Appl. Phys. Lett.* **49** (1986) 1151.
97. R. W. ALEXANDER, R. J. BELL and C. A. WARD, 'Electromagnetic Surface Modes', (Wiley, 1982) Edited by A. D. Boardman, Ch. 5.
98. W. KNOLL, M. R. PHILPOTT, J. D. SWALEN and A. GIRLANDO, *J. Chem. Phys.* **77** (1982) 2254.
99. C. DUSCHL and W. KNOLL, *J. Phys. Chem.* **88** (1988) 4062.
100. H. KNOBLOCH, C. DUSCHL and W. KNOLL, *J. Phys. Chem.* **91** (1989) 3810.
101. R. K. CHANG and T. E. FUTAK (Ed), 'Surface Enhanced Raman Scattering', (Plenum, New York, 1982).
102. V. I. SILIN, S. A. VORONOV, V. A. YAKOVLEV and G. N. ZHIZHIN, *Inter. J. Infrared and Millimeter Waves* **10** (1989) 101.
103. M. KUIJK and R. VOUNCKX, *J. Appl. Phys.* **66** (1989) 1544.
104. G. I. STEGEMAN, A. A. MARADUDIN and R. F. WALLIS, *J. de Phys.* **C5** (1984) 233.
105. A. D. BOARDMAN and T. TWARDOWSKI, *IOP Short Meetings Series Number 9: Surface Plasmon-Polaritons*, (1988) 101.
106. J. D. SWALEN and M. R. PHILPOTT, *J. Chem. Phys.* **69** (1978) 2912.
107. J. D. SWALEN, I. POCKRAND, J. G. GORDON II and M. R. PHILPOTT, *J. Chem. Phys.* **70** (1979) 3401.
108. A. BRILLANTE, I. POCKRAND, M. R. PHILPOTT and J. D. SWALEN, *Chem. Phys. Lett.* **57** (1978) 395.
109. I. POCKRAND, A. BRILLANTE, M. R. PHILPOTT and J. D. SWALEN, *Opt. Comm.* **27** (1978) 91.
110. R. F. WALLIS, A. D. BOARDMAN and M. SHABAT, 'Nonlinear Waves in Solid State Physics', (Erice, Sicily, 1989) to be published.
111. R. H. RITCHIE, E. T. ARAKAWA, J. J. COWAN and R. N. HANN, *Phys. Rev. Lett.* **21** (1968) 1530.
112. M. C. HUTLEY, 'Diffraction Gratings' (Academic Press, 1982).